Title
Energy Dependence of Multiplicity Distributions in the Quantum Statistical Approach

Authors
Fowler, G.N.
Friedlander, E.M.
Navarra, F.S.
et al.

Publication Date
1990-04-01

LBL-28956
Preprint

Lawrence Berkeley Laboratory

UNIVERSITY OF CALIFORNIA

Submitted to Journal of Physics G

Energy Dependence of Multiplicity Distributions in the Quantum Statistical Approach

G.N. Fowler, E.M. Friedlander, F.S. Navarra,
F.W. Pottag, R.M. Weiner, and G. Wilk

April 1990

Prepared for the U.S. Department of Energy under Contract Number DE-AC03-76SF00098.

DISCLAIMER

LBL - 28956

Energy Dependence of Multiplicity Distributions in the Quantum Statistical Approach

G.N. Fowler, E.M. Friedlander, F.S. Navarra, F.W. Pottag,
R.M. Weiner and G. Wilk

April 1990

This work was supported by the Director, Office of Energy Research, Division of Nuclear Physics of the Office of High Energy and Nuclear Physics of the U.S. Department of Energy under Contract DE-AC03-76SF00098

Energy Dependence of Multiplicity Distributions in the Quantum Statistical Approach

G.N. Fowler[1], E.M. Friedlander[2], F.S. Navarra[3a], F.W. Pottag[2,3], R.M. Weiner[3] and G. Wilk[4]

1 University of Exeter, Great Britain, UK
2 Nuclear Science Division, Lawrence Berkeley Laboratory, University of California, CA 94720, USA
3 Department of Physics, University of Marburg, FRG
4 Soltan Institute of Nuclear Studies, Warsaw, Poland
a Present address: Department of Physics, University of São Paulo, Brazil

PACS: 1385 1240E

Abstract

In the quantum statistical approach to the study of multiplicity distributions the most relevant variables are the amount of chaoticity of the source, the coherence length of the fields, and the mean multiplicity. We investigate the energy dependence of these quantities as it appears from the available data in the range 24 GeV $\leq \sqrt{s} \leq$ 900 GeV, by considering also the effect of inelasticity. The main result is that chaoticity as well as coherence length increase significantly with the primary energy. Extrapolations to $\sqrt{s} = 2000$ GeV and 40000 GeV, for the first five moments of the multiplicity distribution and for the forward-backward correlation become possible.

In a previous work [1] quantum statistics (QS) was applied to the study of multiplicity distributions from high energy hadronic collisions measured in finite rapidity windows. Among other things a new scaling property in rapidity ("beta-scaling") was derived, in terms of which the multiplicity distributions $P(n)$ in finite rapidity windows and the forward-backward correlation of multiplicities in the entire available energy range could be understood. The essential parameters of the QS formalism are [1]:

1. $< n >$: the mean multiplicity. Its values are determined in experiment and used as input in the QS parametrizations;
2. p : the amount of chaoticity;
3. β : the ratio between Y, the effective width of the rapidity window * and ξ, the correlation length of the chaotic component of the π fields.

These parameters contain all the dynamical information of the system; in ref.[1] we obtained evidence that p increases with the c.m.s. energy $\sqrt{s}$. Because of the fact that only two energies were considered, no conclusion about the energy dependence of ξ could be drawn and no functional dependence of p on s could be obtained. Furthermore the role of inelasticity on $P(n)$ was not considered in ref.[1]. In the present paper, by considering eight different energies in the CERN-ISR and $p\overline{p}-$Collider range (23.9 GeV $\leq \sqrt{s} \leq$ 900 GeV) a much clearer picture on the s dependence emerges. We find that not only p, but also ξ increases with energy and that the s dependence of ξ is even stronger than that of p. Several assumptions about the functional dependence of $< n >$, p and ξ on the energy W effectively used

*i.e. the width of the Y interval over which the physics (rapidity density, chaoticity, etc.) can be assumed stationary.

for particle production have been investigated; predictions based on the observed trends, are made for $\sqrt{s} = 2000$ GeV where, as yet, no multiplicity distribution was reported and 40000 GeV, the energy of the projected SSC machine.

Quantum statistics and in general most theoretical approaches refer to physical quantities at a fixed energy available for particle production:

$$W = K\sqrt{s} \tag{1}$$

where K is the inelasticity, a quantity which, generally speaking, varies from event to event with a probability density $\chi(K)$. On the other hand measurements are usually made at fixed s which means that the data are actually averaged over the distribution $\chi(K)$. The relation between the "intrinsic" conditional probability $P(n|K,s)$ that in a certain event at a center of mass energy $\sqrt{s}$ and inelasticity K a number n of secondaries be created and the experimentally measured multiplicity distribution $P_{exp}(n)$ is:

$$P_{exp}(n) = \int_0^1 dK\, \chi(K)\, P(n|K,s) \quad . \tag{2}$$

It is usually $P(n|K,s)$ and/or its moments at a given W (i.e. at given K) to which theoretical models, and in particular QS, refer. To perform the integral (2) the dependence of $P(n|K,s)$ on K, has to be known. In the variant of QS discussed in ref.[1] and considered also in the present paper, there exist analytical expressions for the factorial cumulants μ_r rather than for $P(n|K,s)$. Our strategy will then be to express the physical observables in terms of the μ_r (cf. eqs.(14)- (16)) and then compare with QS. These observables are the moments of the multiplicity distribution

$$C_r = \frac{< n^r >}{< n >^r}$$

and the slope b of the forward-backward (F-B) asymmetry given by

$$< n_F >= a + b n_B \tag{3}$$

where n_F and n_B are the number of particles observed in the forward and backward hemisphere respectively.

We express now, using the QS formalism of ref.[1] C_r and b in terms of μ_r and $\mu_{r,F}$ where $\mu_{r,F}$ refers to the forward hemisphere (it is obtained from μ_r by the substitutions $Y \to Y/2 \quad , \quad <n> \to <n_F> = <n>/2$).

The K dependence of μ_r comes in through the W dependence of β, $<n>$ and p; with this in mind we write $\mu_r(K,s)$ as:

$$\mu_r(K,s) = (r-1)! <n>^r \left\{ p^r \cdot B_r(\beta) + r \cdot p^{r-1} \cdot (1-p) \cdot \tilde{B}_r(\beta) \right\} \tag{4}$$

where $<n> = <n>(W,s)$, $p = p(W,s)$, $\beta = \beta(W,s)$ and the first five functions $B_r(\beta)$ and $\tilde{B}_r(\beta)$ are [2]:

$$\begin{aligned}
B_1(\beta) &= 1 \\
B_2(\beta) &= \frac{1}{2}(e^{-2\beta} + 2\beta - 1)\beta^{-2} \\
B_3(\beta) &= \frac{3}{2}((\beta+1)e^{-2\beta} + \beta - 1)\beta^{-3} \\
B_4(\beta) &= \frac{1}{8}(e^{-4\beta} + 4(4\beta^2 + 10\beta + 7)e^{-2\beta} + 20\beta - 29)\beta^{-4} \\
B_5(\beta) &= \frac{5}{24}(3(\beta+1)e^{-4\beta} + 4(2\beta^3 + 9\beta^2 + 15\beta + 9)e^{-2\beta} + \\
&+ 21\beta - 39)\beta^{-5}.
\end{aligned} \tag{5}$$

$$\begin{aligned}
\tilde{B}_1(\beta) &= 1 \\
\tilde{B}_2(\beta) &= 2(e^{-\beta} + \beta - 1)\beta^{-2} \\
\tilde{B}_3(\beta) &= (-e^{-2\beta} + 2(\beta+4)e^{-\beta} + 4\beta - 7)\beta^{-3} \\
\tilde{B}_4(\beta) &= \frac{1}{2}(e^{-3\beta} - 2(2\beta+5)e^{-2\beta} + (2\beta^2 + 18\beta + 47)e^{-\beta} + 16\beta - 38)\beta^{-4} \\
\tilde{B}_5(\beta) &= \frac{1}{12}(-3e^{-4\beta} + 18(\beta+2)e^{-3\beta} - 12(2\beta^2 + 11\beta + 17)e^{-2\beta} + \\
&+ 2(2\beta^3 + 30\beta^2 + 171\beta + 366)e^{-\beta} + 192\beta - 561)\beta^{-5}
\end{aligned} \tag{6}$$

We have tried several parametrizations for the W (and s) dependence of $<n>$, p

and β as listed in Table 1a. Common to these is that:

$$< n > (W, s) = u_n \, W^{v_n} \tag{7}$$

for which there exists both the long-standing prediction ($s^{1/4}$) of the thermodynamical-hydrodynamical models [3, 4, 5] as well as some empirical support [6]. For p and β the parametrizations may be justified aposteriori. We then determine the 3 pairs of parameters $(u_n, v_n), (u_p, v_p)$ and (u_β, v_β) by a simultaneous best fit of eq.(7) and the parametrizations for p and β given in Table 1a to the experimentally measured $\overline{< n >}_{ch}(s)$, $C_2(s)$ and the FB correlation parameter b. (For physical reasons u_n, v_n, u_p and u_β are chosen positive.) These quantities are given by

$$\overline{< n >}(s) = \int_0^1 dK \, \chi(K, s) \, < n > (W(K), s) \tag{8}$$

$$C_2(s) = \frac{\overline{< n^2 >}}{\overline{< n >}^2} = \frac{\overline{\mu_2} + \overline{< n >} + \overline{< n >^2}}{\overline{< n >}^2} \tag{9}$$

and

$$b(s) = \frac{\overline{< n_F n_B >} - \overline{< n_F >}^2}{\overline{< n_F^2 >} - \overline{< n_F >^2}} = \frac{\frac{1}{2}\overline{\mu}_2 - \overline{\mu}_{2,F} + \Delta}{\overline{\mu}_{2,F} + \frac{1}{2}\overline{< n >} + \Delta} \tag{10}$$

where

$$\Delta = \frac{1}{4}\left(\overline{< n >^2} - \overline{< n >}^2\right)$$

and the bar denotes an averaging over $\chi(K, s)$. For more simplicity of notation we will hereafter drop this bar (except of course in eqs.(14)-(16)) but keep in mind that experimental inputs are always averaged over $\chi(K, s)$.

A closed analytical expression for $\chi(K, s)$ has been derived [7, 8]; in order to simplify the calculations one may replace it in zero order approximation by a delta function with the same mean value $\overline{K}$:

$$\chi(K, s) = \delta\left(K - \overline{K}(s)\right) \tag{11}$$

Numerical calculations have however been done with $\chi(K,s)$ according to ref. [7, 8] too.

The simultaneous fit to all available data [9, 10, 11, 12, 13], was done using the standard MINUIT program. Table 1b gives the estimate values for the parameters (u_n, v_n), (u_p, v_p), (u_β, v_β), for all tried parametrizations in Table 1a; the trends of p and ξ for parametrization #1 are illustrated by figs. 1 and 2 which show the rise of both parameters as well as values extrapolations to $\sqrt{s} = 2$ and 40 TeV. Although all parametrizations of Table 1a yield acceptable fits over the s-interval covered by presently available experimental data, parametrization #1 provides the smoothest extrapolation beyond this range, the most stable solution in the optimization procedure and the smallest errors for the extrapolations. The errors were obtained by Monte Carlo simulations.

The values of the correlation length quoted were obtained by approximating the effective rapidity range for different energies as follows:

$$|Y| \sim 0.036 + 0.79 \ln \sqrt{s} \qquad (\sqrt{s} \text{ in GeV}). \tag{12}$$

We observe that the amount of chaoticity p increases with energy; at the same time the parameter β defined as the ratio between Y (the effective rapidity range) and ξ (the effective correlation length of the chaotic component of the emitter) decreases with energy. Since the width Y of the flat part of the rapidity spectrum is known up to 1 TeV (and these data have been used in Tables 2 and 3), one can derive therefrom the variation of ξ; using eq.12 as a reasonable extrapolation of Y into the, as yet, unmeasured s-region we obtain predictions for ξ.

It is important to notice that the correlation length ξ is a field correlation length for which the multiplicity n is not specified. This field correlation length is not to be confused with the rapidity correlation length as used e.g. in ref.[8] where measurements were made at fixed n in order to eliminate irrelevant correlations arising from energy momentum conservation. It is fundamental to the field point of view that the effect of conservation laws should be negligible so that the quantity ξ is a correlation length with n unrestricted by the rapidity limited to the central region.

Note that eq.(7) refers to the *total* multiplicity $< n >$ of produced secondaries; neglecting non-pions among the produced secondaries and assuming charge persistence on the leading baryons the mean *charged* multiplicity is then

$$< n >_{ch} = \frac{2}{3} < n > + 2. \tag{13}$$

In fig. 3 we show the s-dependence of $< n >_{ch}$ according to both the power law (eq.7) and the quadratic $\ln s$ fit used in ref.[10]. The choice of the fit for $< n >_{ch}$ lies outside the scope of the QS approach. With the parameters u_α, v_α (where α is either n, p or β) obtained above we go back to expressions (8)-(10) and calculate $< n >_{ch}$, C_2 and b at $\sqrt{s} = 2$ TeV and 40 TeV. The higher C_r moments can also be calculated using the formulae:

$$C_3 = \frac{\overline{\mu_3} + 3\overline{\mu_2\,\mu_1} + \overline{\mu_1^3} + 3\overline{\mu_2} + 3\overline{\mu_1^2} + \overline{\mu_1}}{\overline{\mu_1}^3} \tag{14}$$

$$\begin{aligned} C_4 &= \frac{\overline{\mu_4} + 4\overline{\mu_1\,\mu_3} + 3\overline{\mu_2^2} + 6\overline{\mu_1^2\,\mu_2} + \overline{\mu_1^4}}{\overline{\mu_1}^4} + \\ &+ \frac{6\overline{\mu_3} + 18\overline{\mu_1\,\mu_2} + 6\overline{\mu_1^3} + 7\overline{\mu_2} + 7\overline{\mu_1^2} + \overline{\mu_1}}{\overline{\mu_1}^4} \end{aligned} \tag{15}$$

$$\begin{aligned} C_5 &= \frac{\overline{\mu_5} + 5\overline{\mu_1\,\mu_4} + 10\overline{\mu_2\,\mu_3} + 10\overline{\mu_1^2\,\mu_3} + 15\overline{\mu_1\,\mu_2^2} + 10\overline{\mu_1^3\mu_2}}{\overline{\mu_1}^5} + \\ &+ \overline{\mu_1^5} + 10\overline{\mu_4} + 40\overline{\mu_1\,\mu_3} + 30\overline{\mu_2^2} + 60\overline{\mu_1^2\,\mu_2} + 10\overline{\mu_1^4} + \\ &+ \frac{25\overline{\mu_3} + 75\overline{\mu_1\,\mu_2} + 25\overline{\mu_1^3} + 15\overline{\mu_2} + 15\overline{\mu_1^2} + \overline{\mu_1}}{\overline{\mu_1}^5} \end{aligned} \tag{16}$$

The results are shown in fig. 4 which includes also extrapolations from the negative binomial [10].

We mentioned above that the results for $< n >_{ch}$, p and ξ depend little, if at all, on whether a constant full inelasticity $K = 1$ or a variable mean inelasticity was assumed. Within the energy range used for the fits this is obvious (it only confirms the goodness of the fit !). The extrapolation to the energy domain of the Tevatron and *a fortiori* the SSC is an entirely different matter. The fact that the two sets of extrapolations differ by not much more than the statistical errors attached to the extrapolation is far from trivial. It follows only in part from the smallness of the exponents v (which will tend to weaken s-dependences); an important ingredient is the reliance upon the (far from certain) extrapolations of $\overline{K}$ deduced from the model of ref.[7, 8]. One might, e.g. assume that the falling trend of $\overline{K}$ with s ceases beyond $\sqrt{s} = 1$ TeV; then quite different predictions would occur (e.g. at the SSC $< n >_{ch}$=210 instead of 165 !). An opposite extreme assumption about the asymptotic behaviour of $< n >_{ch}$ could be to accept the fits to cross-sections in very high energy cosmic ray events [14, 15] which lead to $\overline{K} \sim s^{-0.14}$. This would imply $< n >_{ch}$= 109 at SSC energies.

For the sake of comparison we also give in Table 4 the predictions based on the extrapolation of the negative binomial fit used by the UA5 collaboration [10].

The new results of this investigation can thus be summarized as follows: Not only the chaoticity p but also the coherence length ξ increase with energy. This trend is not influenced by the inelasticity and is robust with respect to parametrization of the s-dependence.

This work was supported in part by the Federal Minster for Research and Technology (BMFT) under the contract number 06 MR 777 and the Gesellschaft für Schwerionenforschung Darmstadt. E.M. Friedlander was supported by the Director, Office of Energy Research, Office of High Energy and Nuclear Physics, Nuclear Physics

Division of the U.S. Department of Energy under Contract DE-AC03-76SF00098. F.W. Pottag was supported by a Feodor Lynen fellowship of the Alexander von Humboldt Foundation.

References

[1] G.N. Fowler et al., Phys. Rev. D37, 3127 (1988).

[2] C.C. Shih, Phys. Rev. A40, 1456 (1989).

[3] E. Fermi, Prog. Theor. Phys. 5, 570 (1950).

[4] E. Fermi, Phys. Rev. 81, 683 (1951).

[5] Collected Papers of L.D. Landau, edited by Ter Haar, Gordon & Breach, N.Y., 569 (1965).

[6] D. Brick et al., Phys. Lett. 103B, 242 (1981). Note that in the Landau hydrodynamical model this parametrization is not fullfilled even if one generalizes this model by assuming that the mass of the expanding system depends only on W and not on s. This is so because the Lorentz contraction which determines the volume of the system and thus the available initial energy density, depends on s. (For a more detailed discussion of this topic cf. R.M. Weiner, Hadronic Matter Under Extreme Conditions, Vol. 2, Editors: Zinoviev and Shelest, Kiev Naukova Dumka, 1986).

[7] G.N. Fowler et al., Phys. Rev. D35, 870 (1987).

[8] G.N. Fowler et al., Phys. Rev. C40, 1219 (1989).

[9] S. Uhlig et al., Nucl. Phys. B132, 15 (1978).

[10] UA5, G.J. Alner et al., Phys. Lett. 160B, 199 (1985).

[11] UA5, G.J. Alner et al., Phys. Rep. 154, 247 (1987).

[12] UA5, R.E. Ansorge et al., Z. Phys. C37, 191 (1988).

[13] UA5, R.E. Ansorge et al., Z. Phys. C43, 357 (1989).

[14] T. Stanev and G.B. Yodh, Hadronic Multiparticle Production, World Scientific, edited by P. Carruthers, 289, (1988).

[15] P. Carlson, Proc. of European Cosmic Ray Symposium, Bordeaux, France, edited by J.N. Capdevielle, 149, (1986).

Table Captions

Table 1a

Parametrizations used for the W dependence of p and β; the one used for $< n >$ is the same in all cases and given by eq.(7).

Table 1b

Estimates for the parameters of the parametrizations described in Table 1a. The last row shows the χ^2 values for 18 degrees of freedom.

Table 2

Effective energy (W), and estimates for p (chaoticity), β, ξ (the correlation length), and $< n >_{ch}$ (the mean charged multiplicity). The values for 2 TeV and 40 TeV are extrapolations.

Table 3

Estimate values of: b (the forward-backward correlation slope), and moments C_r of the multiplicity distribution. The values for 2 TeV and 40 TeV are extrapolations.

Table 4

Predictions of the C_q based on the extrapolation of the negative binomial fit used by the UA5 Collaboration [10].

Figure Captions

Fig. 1

s-dependence of p according to fits done with parametrization #1 of Table 1a (this parametrization was used in all subsequent figures). Errors are shown for values extrapolated to 2 TeV and 40 TeV.

Fig. 2

s-dependence of the correlation length ξ. Errors are shown for values extrapolated to 2 TeV and 40 TeV.

Fig. 3

s-dependence of $< n >_{ch}$. Experimental data are shown as diamonds; extrapolations according to eq.(7) are shown as asterisks; extrapolations according to the quadratic expression in $\ln s$ used in ref.[10] are shown as squares.

Fig. 4

s-dependence of normalized initial moments C_q of the charged multiplicity distribution for q=2,...,5. Symbols are the same as in Fig. 3.

Table 1a

#	1	2	3	4
$p(W,s)$	$u_p \ln(W) + v_p$	$u_p \ln(W) + v_p$	$1 - \exp(-u_p \exp(W^{v_p}))$	$1 - \exp(-u_p W^{v_p})$
$\beta(W,s)$	$u_\beta W^{-v_\beta}$	$u_\beta \exp(-W^{v_\beta})$	$u_\beta \exp(-W^{v_\beta})$	$u_\beta W^{-v_\beta}$

Table 1b

#	1	2	3	4
u_p	0.031 ± 0.006	0.032 ± 0.007	0.018 ± 0.003	0.038 ± 0.010
v_p	-0.005 ± 0.023	-0.012 ± 0.024	0.15 ± 0.02	0.29 ± 0.06
u_β	6.5 ± 1.2	11.7 ± 1.5	11.5 ± 1.6	6.2 ± 1.2
v_β	0.33 ± 0.04	0.16 ± 0.01	0.16 ± 0.01	0.32 ± 0.04
u_n	3.6 ± 0.1	3.6 ± 0.1	3.6 ± 0.1	3.6 ± 0.1
v_n	0.48 ± 0.01	0.48 ± 0.01	0.48 ± 0.01	0.48 ± 0.01
$\chi^2(\nu = 18)$	15.2	14.4	15.3	14.9

Table 2

$\sqrt{s}\,(GeV)$	$W\,(GeV)$	p	β	ξ	$< n >_{ch}$
23.9	11.1	0.07 ± 0.01	3.1 ± 0.3	0.8 ± 0.1	9.5 ± 0.1
30.4	14.1	0.07 ± 0.01	2.8 ± 0.3	1.0 ± 0.1	10.4 ± 0.1
44.5	20.5	0.08 ± 0.01	2.5 ± 0.2	1.2 ± 0.1	12.0 ± 0.1
52.6	24.0	0.09 ± 0.01	2.4 ± 0.2	1.4 ± 0.1	12.8 ± 0.1
62.6	28.2	0.09 ± 0.01	2.3 ± 0.1	1.5 ± 0.1	13.7 ± 0.1
200	77	0.12 ± 0.01	1.6 ± 0.1	2.6 ± 0.1	20.9 ± 0.2
546	176	0.15 ± 0.01	1.3 ± 0.1	4.1 ± 0.2	29.9 ± 0.4
900	264	0.16 ± 0.01	1.1 ± 0.1	5.1 ± 0.3	35.9 ± 0.6
2000	508	0.18 ± 0.02	0.9 ± 0.1	7.0 ± 0.5	48.4 ± 1.0
40000	6480	0.27 ± 0.03	0.4 ± 0.1	23 ± 4	165 ± 7

Table 3

$\sqrt{s}\,(GeV)$	b	C_2	C_3	C_4	C_5
23.9	0.20 ± 0.01	1.20 ± 0.01	1.65 ± 0.02	2.6 ± 0.1	4.4 ± 0.1
30.4	0.23 ± 0.01	1.20 ± 0.01	1.65 ± 0.02	2.6 ± 0.1	4.5 ± 0.1
44.5	0.28 ± 0.01	1.20 ± 0.01	1.67 ± 0.02	2.6 ± 0.1	4.7 ± 0.1
52.6	0.30 ± 0.01	1.20 ± 0.01	1.69 ± 0.02	2.7 ± 0.1	4.8 ± 0.1
62.6	0.32 ± 0.01	1.21 ± 0.01	1.70 ± 0.02	2.7 ± 0.1	4.9 ± 0.1
200	0.48 ± 0.01	1.24 ± 0.01	1.84 ± 0.04	3.2 ± 0.1	6.3 ± 0.4
546	0.59 ± 0.01	1.28 ± 0.01	2.01 ± 0.06	3.8 ± 0.2	8.1 ± 0.7
900	0.64 ± 0.01	1.30 ± 0.02	2.11 ± 0.07	4.1 ± 0.2	9.3 ± 0.8
2000	0.70 ± 0.01	1.34 ± 0.02	2.3 ± 0.1	4.7 ± 0.3	11 ± 1
40000	0.85 ± 0.02	1.39 ± 0.04	2.6 ± 0.2	6 ± 1	18 ± 4

Table 4

$\sqrt{s}\,(TeV)$	C_2	C_3	C_4	C_5
2	1.36 ± 0.02	2.32 ± 0.07	4.77 ± 0.25	11.50 ± 0.90
40	1.51 ± 0.02	3.07 ± 0.10	7.77 ± 0.44	24 ± 2

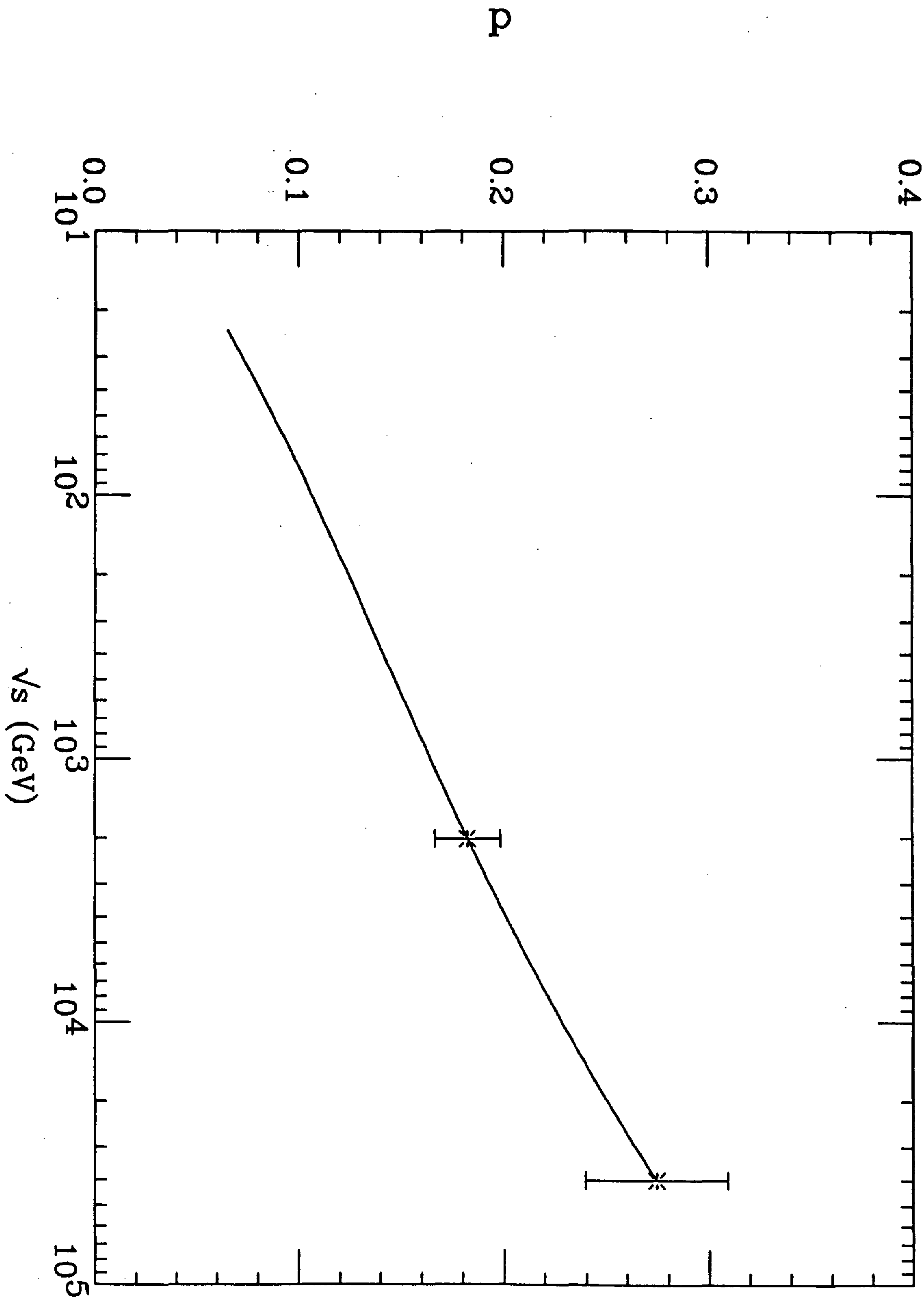

Fig−1

Fig-2

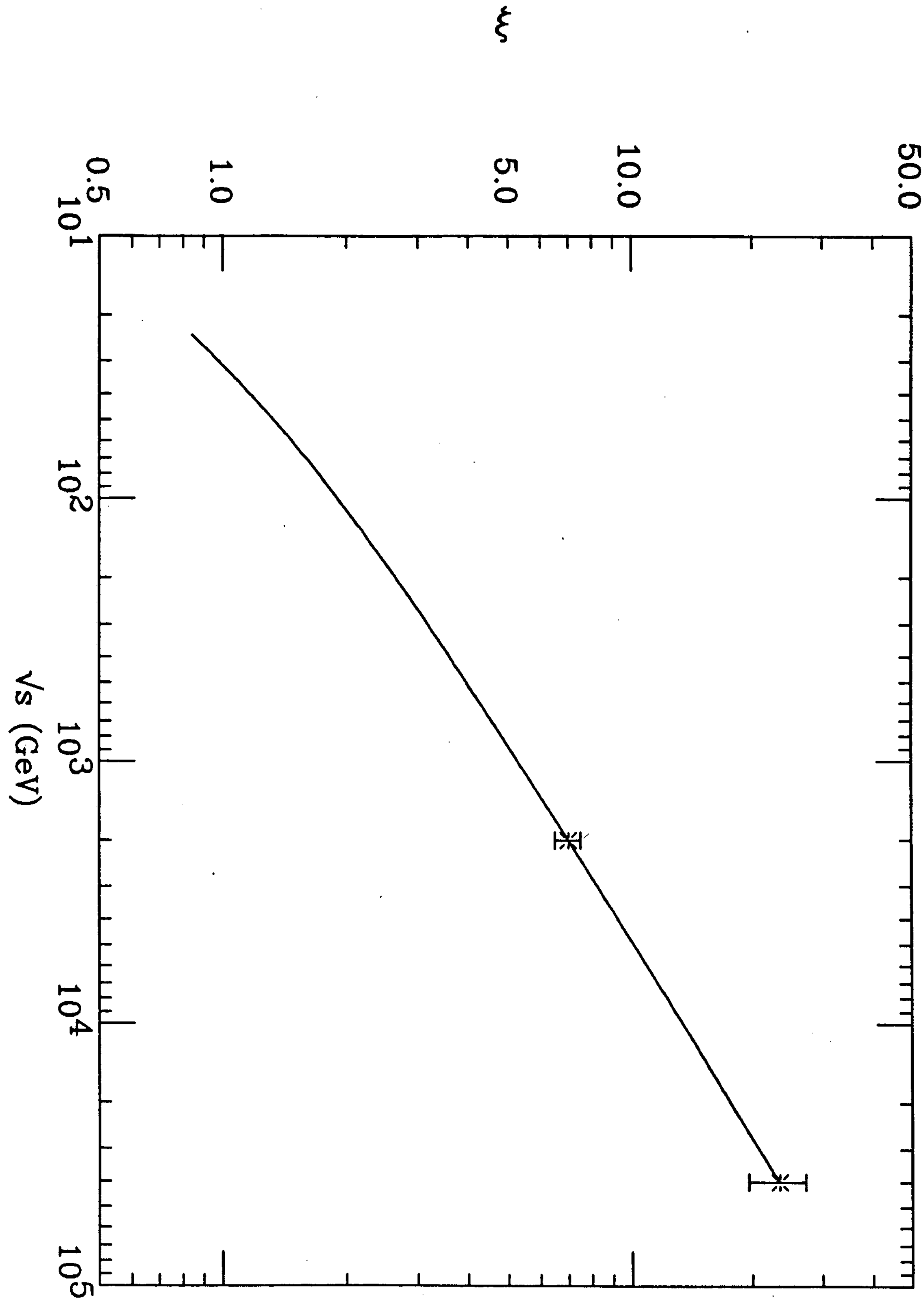

Fig-3

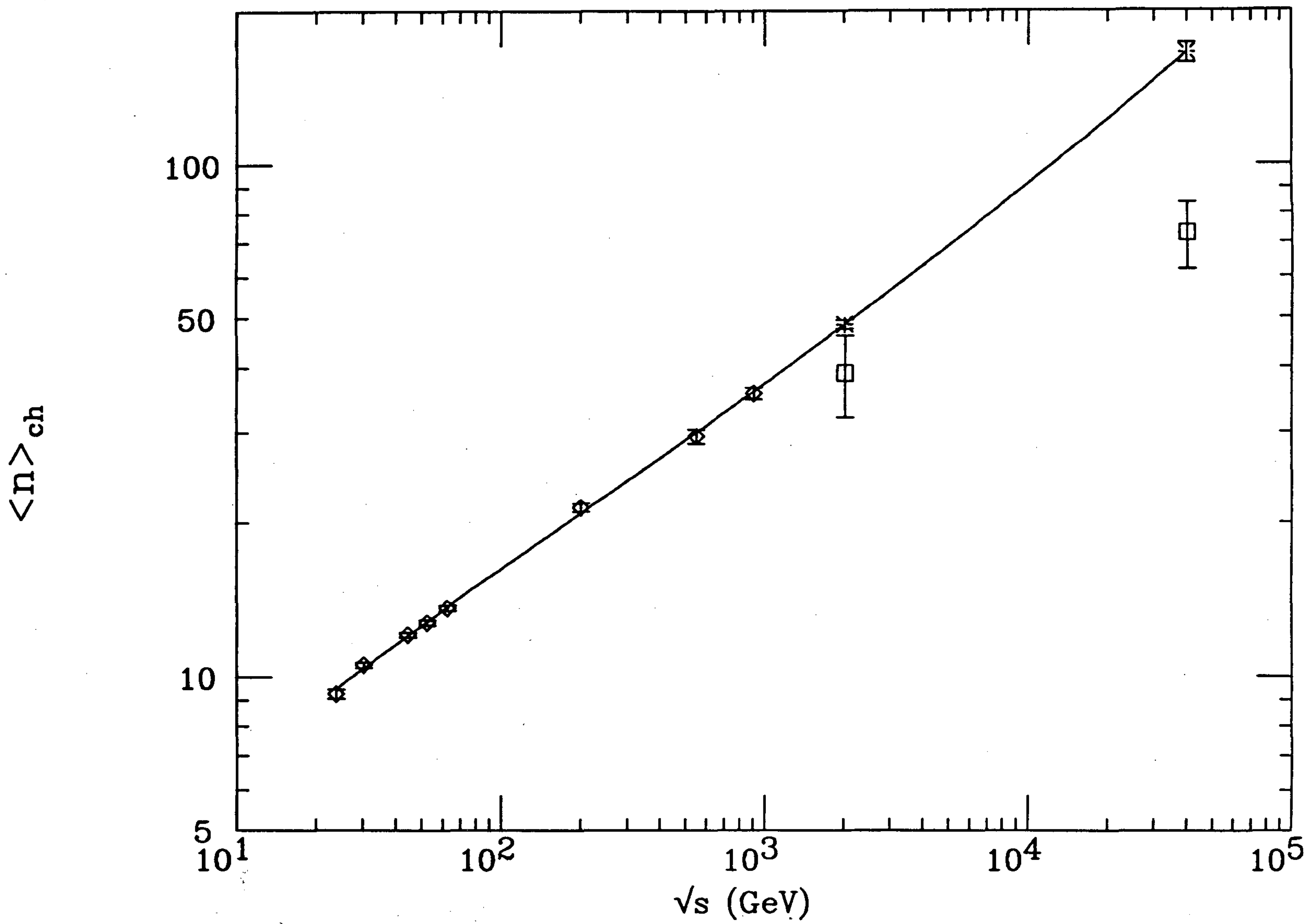

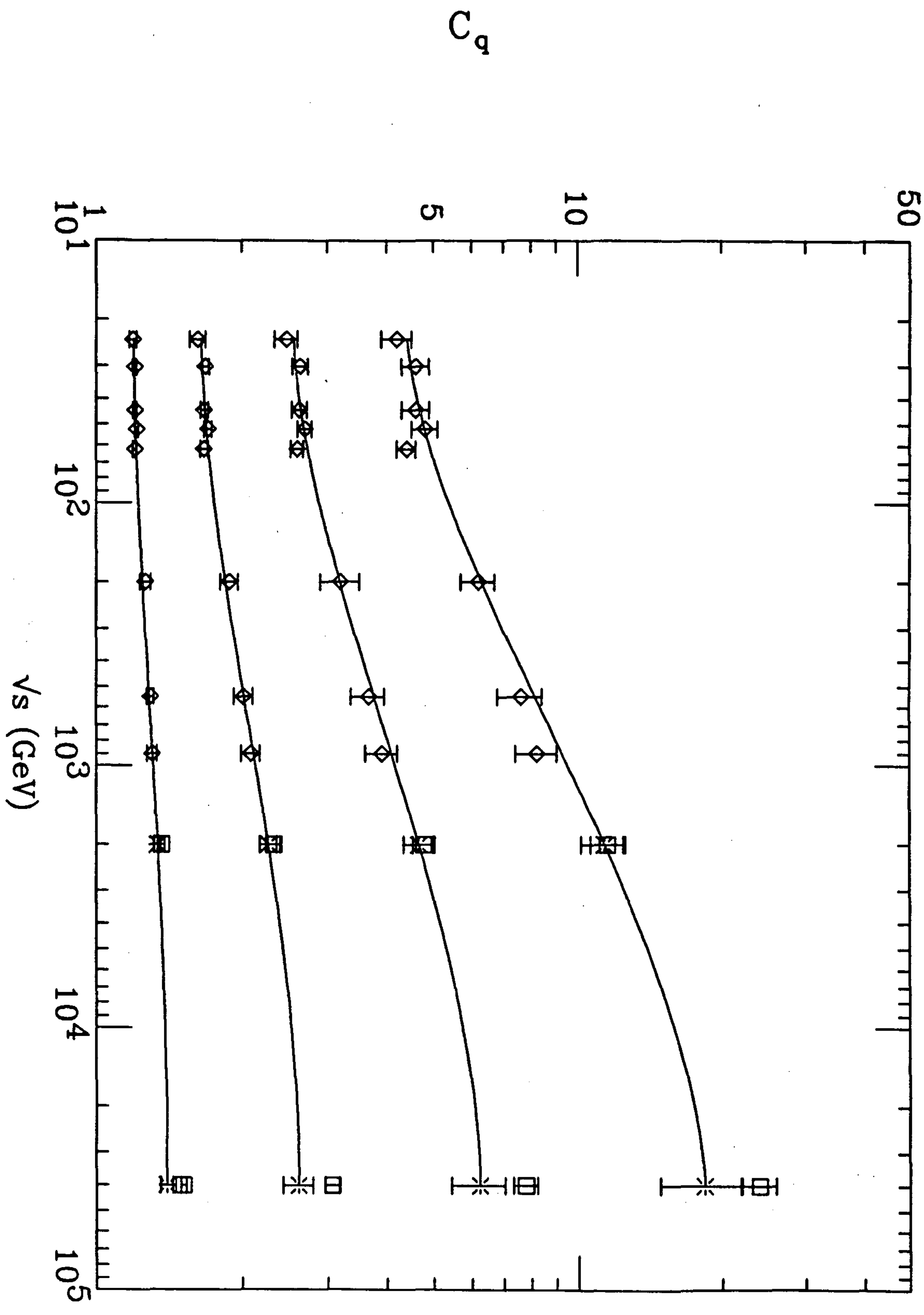

Fig−4

LAWRENCE BERKELEY LABORATORY
UNIVERSITY OF CALIFORNIA
INFORMATION RESOURCES DEPARTMENT
BERKELEY, CALIFORNIA 94720